Catalysis Today xxx (xxxx) xxx–xxx

Contents lists available at ScienceDirect

Catalysis Today

journal homepage: www.elsevier.com/locate/cattod

Strong interaction between Au nanoparticles and porous polyurethane sponge enables efficient environmental catalysis with high reusability

Qijie Jin[a,b,1], Lei Ma[a,1], Wan Zhou[a], Ramana Chintalapalle[c], Yuesong Shen[b,*], XiuJun Li[a,d,**]

[a] Department of Chemistry and Biochemistry, University of Texas at El Paso, El Paso, Tx, 79968, USA
[b] College of Materials Science and Engineering, Nanjing Tech University, Nanjing 210009, China
[c] Department of Mechanical Engineering, University of Texas at El Paso, El Paso, Tx, 79968, USA
[d] Environmental Science and Engineering,Biomedical Engineering, Border Biomedical Research CenterUniversity of Texas at El Paso, El Paso, Tx, 79968, USA

ARTICLE INFO

Keywords:
Environmental degradation
Au nanoparticles
Polyurethane sponge
Catalysis reduction
Nitroaromatic compounds

ABSTRACT

A novel and recoverable platform of polyurethane (PU) sponge-supported Au nanoparticle catalyst was obtained by a water-based in-situ preparation process. The structure, chemical, and morphology properties of this platform were characterized by XRD, TGA, SEM, FT-IR, and XPS. The Au/PU sponge platform exhibited excellent catalytic performances in catalytic reductions of *p*-nitrophenol and *o*-nitroaniline at room temperature, and both catalytic reactions could be completed within 4.5 and 1.5 min, respectively. Furthermore, the strong interaction between Au nanoparticles and the PU sponge enabled the catalyst system to maintain a high catalytic efficiency after 5 recycling times, since the PU sponge reduced the trend of leaching and aggregation of Au nanoparticles. The unique nature of Au nanoparticles and the porous PU sponge along with their strong interaction resulted in a highly efficient, recoverable, and cost-effective multifunctional catalyst. The AuNP/Sponge nanocatalyst platform has great potential for wide environmental and other catalytic applications.

1. Introduction

Noble metal nanoparticles (NPs) have attracted growing attention in various fields including catalysis, environmental remedy, biomass conversion, and biomedical applications [1–4], due to their unique size and shape effect [5–9]. As an example, nano palladium-based catalysts have been applied for various organic reactions, such as primary amides synthesis and oxidative amidation reactions [10–12]. Because of the isoelectronic nature and acidic character of gold with palladium species, researchers have extensively investigated Au nanomaterials [13,14]. Hashmi explained the role of Au nanoparticles (AuNPs) for organic transformations toward heterogeneous catalysis [15]. Thereafter, Au nanocatalysts have been applied for tremendous fields of organic transformation, including nitroaromatic compounds reduction [16,17], CO oxidation [18,19], carbon-carbon coupling reactions [20,21], and so on. To decompose nitroaromatic compounds for environmental remedy, catalysts need to meet several vital requirements before their industrial and other practical applications: (1) excellent catalytic performance; (2) robust and efficient separation strategy from nitroaromatic compound solutions; (3) long-term stability when immersing in the aqueous phase. However, noble metal nanocatalysts suffer a dilemma to meet these requirements: it is very difficult to increase their catalytic efficiency and reusability simultaneously. Aqueous-phase catalysts can reach high catalytic efficiency, but separation remains a big challenge. Solid-phase catalysts are uncomplicated to separate but their catalytic efficiency is compromised by uneven dispersion. In addition, numerous solid-phase catalysts often become disintegrated in the prolong course when being immersed in water. Despite intensive research, there is still an urgent need to develop novel catalysts with high catalytic efficiency and reusability for nitroaromatic compounds degradation to meet the increasing demand from environmental applications.

The porous polyurethane (PU) sponge, a macromolecule polymer material with long-term stability in water, can serve as a good catalytic carrier. Meanwhile, PU sponge has amino groups on branched chains and its hydrophilicity facilitates catalytic reactions in water. In addition, polymer-based catalysts possess an advantage of facile isolation of products and catalysts can be recovered through a simple re-precipitation/filtration method with proper solvents rather than laborious procedures such as chromatographic separation [22]. Owing to these

* Corresponding author.
** Corresponding author at: Department of Chemistry and Biochemistry, University of Texas at El Paso, El Paso, Tx, 79968, USA.
E-mail addresses: sys-njut@163.com (Y. Shen), xli4@utep.edu (X. Li).
[1] Denotes those authors contribute equally to this work.

https://doi.org/10.1016/j.cattod.2020.01.023
Received 7 March 2019; Received in revised form 17 October 2019; Accepted 19 January 2020
0920-5861/

merits, the PU sponge is an excellent catalytic carrier for the decomposition of nitroaromatic compounds and other catalytic applications. Although PU sponge has been utilized in some catalytic fields such as the removal of methylene blue [23], it has never been used for the nitroaromatic compound catalysis. Furthermore, AuNPs, known as an excellent electron-donor or acceptor, exhibits excellent chemical inertness and could stay stable under various reaction ambiance [24]. Specifically, AuNPs have the potential to promote catalytical reductions of nitroaromatic compounds significantly [25,26]. Therefore, we hypothesize that AuNPs modified PU sponge (AuNP/Sponge) could exhibit excellent catalytic performance to degrade nitroaromatic compounds with high reusability.

It is well known that nitroaromatic compounds, especially *p*-nitrophenol (4-NP) and *o*-nitroaniline (2-NA), are major contributors to worsening environment issues such as water contaminants, which would trigger teratogens, mutagens, and carcinogens [27,28]. Accordingly, a diverse set of nitroaromatic compounds have been encompassed in environmental legislation [29]. On the other hand, *p*-aminophenol (4-AP) and *o*-phenylenediamine (OPD) are crucial intermediates that enable widespread applications in manufacturing fine chemicals and end products, including antipyretic drugs, photographic developer, and corrosion inhibitor [30–32]. The catalytic reduction of nitroaromatic compounds do not only possess great ecological and environmental significance but also important economic values [33,34]. Hence, 4-NP and 2-NA were chosen as model systems to demonstrate the performance of the AuNP/Sponge catalyst for catalytic reduction of nitroaromatic compounds.

Herein, we report a novel high-efficiency and high-reusability AuNP/Sponge catalyst prepared with a facile one-step process for cost-effective catalytic reduction of nitroaromatic compounds. AuNPs were generated on the surface of PU sponge via a water-based in-situ preparation process, because of the strong interaction of AuNPs and PU sponge, and thereafter their catalytic performances in the reduction of 4-NP and 2-NA were systematically studied. The Au/ PU sponge catalyst platform can finish the 4-NP reduction within 4.5 min and 2-NA reduction within 1.5 min, while keeping high catalytic efficiency even after five recycles of catalysis. In addition, their chemical, structure, and morphology properties were characterized by XRD, TGA, SEM, FT-IR, and XPS. The unique properties of Au nanoparticles and the porous PU sponge along with their strong interaction resulted in a highly efficient, recoverable, and cost-effective multifunctional catalyst.

2. Experiment

2.1. Materials

Sodium borohydride ($NaBH_4$, 98 %) was purchased from Alfa Aesar (Tewksbury, MA). *P*-nitrophenol (4-NP) and *o*-nitroaniline (2-NA) were purchased from EMD Millipore Corporation (Billerica, MA). Gold (III) chloride trihydrate ($HAuCl_4{\cdot}3H_2O$) was purchased from Sigma (St. Louis, MO). The polyurethane sponge was purchased from Haofeng, China. Water with a resistivity of 18.2 MΩ.cm@25 °C was from a Millipore Milli-Q system (Bedford, MA). All chemicals were of analytical grade and used without further processing.

2.2. Catalyst preparation

Scheme 1 and Scheme S1 presented the preparation process of the AuNP/Sponge catalyst. The water-based in-situ preparation process was simple and versatile. Firstly, the sponge was cut into the square with a dimension of 1.5 × 1.5 cm^2 (about 75 mg). An appropriate amount of $HAuCl_4{\cdot}3H_2O$ (60 mg, 40 mg, 20 mg, and 10 mg, respectively) was added into 3 mL ultrapure water to obtain a $HAuCl_4$ yellow clarified solution. Secondly, the sponge was compressed to eliminate air bubbles, and in turn, the $HAuCl_4$ solution was absorbed by the sponge. Thirdly, an appropriate amount of $NaBH_4$ was added into 5 mL ultrapure water to obtain a solution. Then, as a mixed precursor, $HAuCl_4$/Sponge was rapidly added into a $NaBH_4$ solution and kept vigorous stirring by a vortex mixer for 30 min to completely reduce Au^{3+}. At last, the resulting black sponge from different amounts of Au ranging from 10 to 60 mg $HAuCl_4{\cdot}3H_2O$ was washed and vacuum dried to obtain a purple AuNP/Sponge catalyst (hereafter denoted as PU sponge, 10AuNP/Sponge, 20AuNP/Sponge, 40AuNP/Sponge, and 60AuNP/Sponge, respectively).

2.3. Catalytic activity measurement

The catalytic efficiency of the AuNP/Sponge platform was investigated by using 4-NP conversion to 4-AP and 2-NA conversion to OPD. As an example of 2-NA conversion to OPD, a quintessential procedure was adopted to carry out the chemical reaction. Firstly, a 2-NA solution (4 mM, 5 mL) and a $NaBH_4$ solution (0.4 M, 5 mL) were added to the conical centrifuge tube (50 mL, Thermo Fisher Scientific, America) and mixed together. Secondly, the AuNP/Sponge platform was placed in a mixed solution and kept vigorous stirring by using a vortex mixer (Thermo Fisher Scientific, America). Afterward, 100 μL mixed solutions were transferred in a 96 well microplate (Thermo Fisher Scientific, America) by using a micropipette. The microplate was placed in a UV–vis spectrophotometer (Microplate reader M3, Molecular Devices, San Jose, CA) to measure its absorbance spectra. The remaining fraction of 2-NA (X) was calculated by the eq (1).

$$X = (C_0\text{-}C_t)/C_0 \times 100\% \quad (1)$$

Where C_0 was the initial 2-NA concentration and C_t was the concentration at different time intervals (t). Furthermore, the AuNP/Sponge catalyst was recycled for 6 times to investigate its reusability. For every recycle, the used catalyst was washed and vacuum dried for the next experiment. A similar procedure was adopted for the 4-NP reduction. The concentrations of 4-NP (1 mM) and $NaBH_4$ (0.1 M) prepared for the experiment were 1 mM and 0.1 M, respectively.

2.4. Characterization

X-ray diffraction (XRD) patterns were obtained on an X-ray diffractometer (Smartlab TM 3Kw, Rigaku, Japan), with a scan speed of $5^{\circ}{\cdot}min^{-1}$ and a 5–80 ° 2θ scan. The microstructural nature of the catalysts was investigated using a field emission instrument scanning electron microscope (S-4800, Hitachi, Japan). Fourier transform infrared (FT-IR) spectra were evaluated by a Nicolet Nexus 670 series FT-IR spectrophotometer in an ATR mode. The spectra were recorded under ambient conditions over the range of $750-4000\ cm^{-1}$ with a resolution of $0.5\ cm^{-1}$. The thermogravimetric analysis was measured by a TGA system (Mettler Toledo International Inc, America). Before the measurement, the sample was dried at 80 °C for 2 h and a ceramic crucible was pre-treated by high-temperature sintering. The 0.5 mg sample was placed in the ceramic crucible and kept on the auto-sample stage of the TGA system. Then, the sample was heated from 30 °C to 1000 °C at a 10 °C min^{-1} heating rate. The gas flow rate of the nitrogen atmosphere was 20 mL·min^{-1}.

3. Results and discussion

3.1. Catalytic reduction of 2-NA

During the catalytic experiment by the Au/PU sponge, the yellow color of a 2-NA/$NaBH_4$ solution faded and bleached ultimately with the addition of the AuNP/Sponge catalyst. The fading time decreased with the increase of the AuNPs amount, and the effect of AuNPs amount was monitored by the UV–vis spectrophotometry. As shown in Figs. 1 and S1, the peak intensity at 410 nm decreased obviously and that at 295 nm decreased slightly with the increasing time. The literature

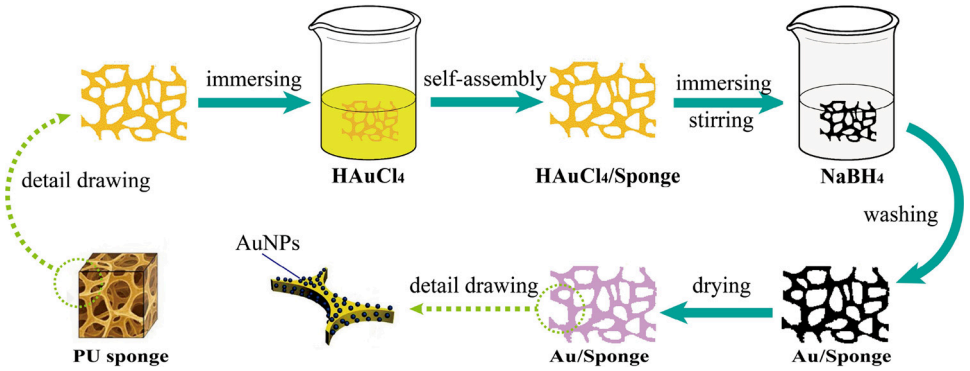

Scheme 1. Preparation of the AuNP/Sponge catalyst.

confirmed that the peak at 410 nm represented 2-NA [35]. Therefore, the change of peak intensity was due to the transformation from 2-NA to OPD when the AuNP/Sponge catalyst was added into the 2-NA/$NaBH_4$ solution. In addition, the peak intensity representing the 2-NA displayed no change in the absence of AuNPs in Fig. S2, suggesting that the PU sponge had no catalytic effect and AuNPs were essential for the catalytic reduction. Furthermore, the conversion rate of the 60AuNP/Sponge could reach 100.0 % within 1 min. The catalytic efficiency decreased gradually when the AuNPs amount reduced. However, the conversion rate of 10AuNP/Sponge could still reach 99.0 % within 1.5 min, indicating excellent performance for the catalytic reduction. In other words, the AuNP/Sponge was an excellent catalyst for catalytic reduction of nitroaromatic compounds.

The catalytic reduction reaction from 2-NA to OPD followed the first-order kinetic because of the excess amount of $NaBH_4$. The kinetic was calculated by Eq. (2).

$$\mathrm{Ln}(C_t/C_0) = -kt \quad (2)$$

Where C_0 was the initial 2-NA concentration, C_t was the concentration at different time intervals (t) and k was the apparent rate constant of the reaction. Fig. 1(b) also displayed the first-order kinetic curves of 2-NA over AuNP/Sponge with different AuNPs amounts. It could be observed that the data points generally followed the linearity, which was due to the vigorous stirring by using a vortex mixer during the period of the catalytic activity measurement. As such, the bubbles produced in the conical centrifuge tube could be eliminated in time. Furthermore, the value of k was 0.0793, 0.0634, 0.0549 and 0.0508 s^{-1}, respectively.

To compare the reusability and determine the optimal catalyst cycles, the used AuNP/Sponge catalysts were washed and vacuum dried for the second recycling time. Fig. S3 displays the UV–vis absorption spectra of 2-NA reduction for a second recycling time and Fig. 2 shows the C_t/C_0 and $\ln(C_t/C_0)$ *vs.* time plot representing first-order kinetics.

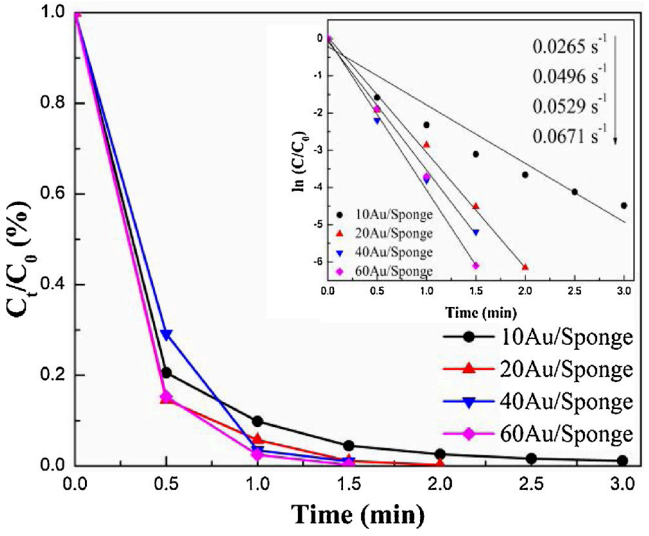

Fig. 2. C_t/C_0 vs. time plot of the 2-NA reduction for a second recycle.

Compared with fresh AuNP/Sponge, all the experiments needed more time to complete the catalytic reduction and the catalytic efficiency decreased slightly. The conversion rate of 60AuNP/Sponge needed 1.5 min to reach 100.0 %, while that of 10AuNP/Sponge reached 98.9 % within 3 min. As generally known, the interaction between AuNPs with PU sponge is a collective effect between chemical bonds and physical adsorption. Accordingly, a small amount of AuNPs physically adsorbed on PU could break off from the PU sponge during the prolong use so that the active component reduced, and the catalytic efficiency decreased gradually. Both conversion rates from 40AuNP/Sponge and 60AuNP/Sponge reached nearly 100.0 % within 1.5 min. Considering

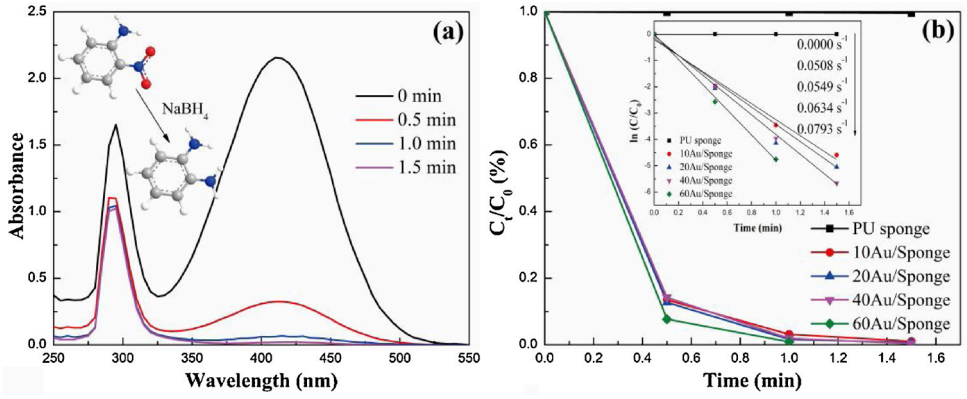

Fig. 1. (a) UV–vis absorption spectra of 2-NA reduction over 40AuNP/Sponge catalyst and (b) C_t/C_0 vs. time plot.

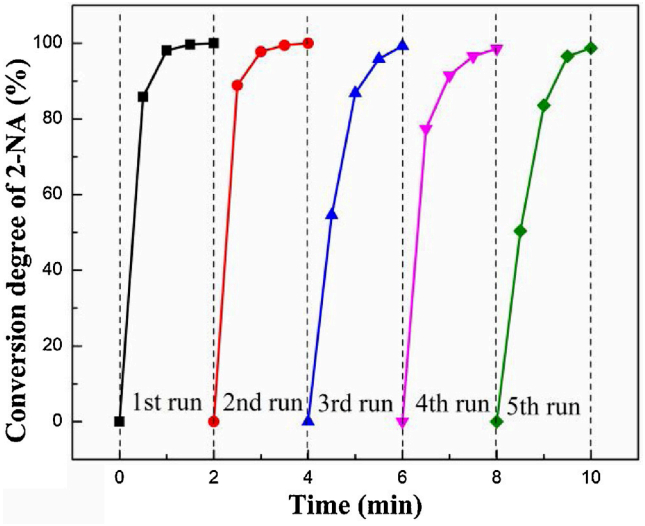

Fig. 3. Effect of recycling time on catalytic reduction of 2-NA over the 40AuNP/Sponge catalyst.

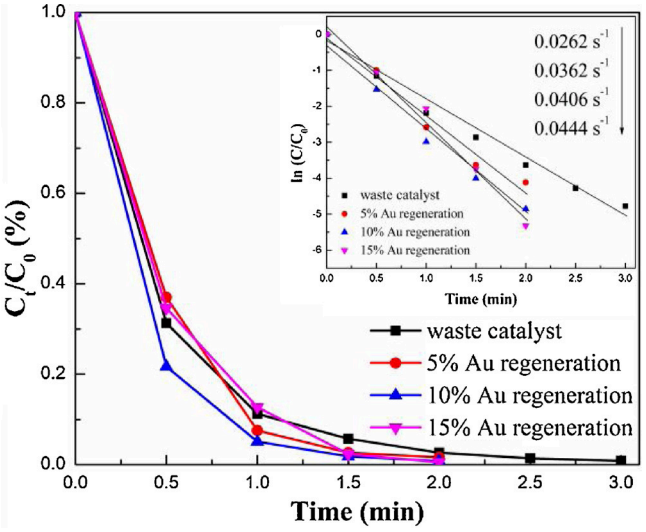

Fig. 4. C_t/C_0 vs. time plot of the 2-NA reduction by the waste catalyst and regenerated catalysts.

that 60AuNP/Sponge had a greater AuNPS loss than 40AuNP/Sponge, the 40AuNP/Sponge as chosen as the optimal catalyst. It can also be seen from Fig. 2 that the data points also followed the linearity, and the value of k was 0.0671, 0.0529, 0.0496 and 0.0265 s^{-1} for the 60AuNP/Sponge, 40AuNP/Sponge, 20AuNP/Sponge, and 10AuNP/Sponge, respectively. They were slightly lower than those K values from fresh AuNP/Sponge.

The major benefits of heterogeneous catalysts are their separation convenience from the reaction medium and reusability in consecutive runs. [36] In the present case, the reusability of 40AuNP/Sponge was investigated in detail (Fig. 3), and the used catalyst was washed and vacuum dried for the subsequent experiments. As shown in Fig. 3 and Fig. S4, all the 2-NA reduction could be completed within 2 min and the declining trend of conversion rate slowed with the increase of the recycling number. It was mainly because there were fewer AuNPs physically adsorbed on the surface of the AuNP/Sponge catalyst. The chemical bond became the dominant interaction between AuNPs and sponge gradually. Furthermore, the conversion rate of the 40AuNP/Sponge catalyst could reach 98.7 % at the fifth recycling time. Compared with other catalysts, such as Cu_2O@h-BN (50 % activity loss after 4 recycling times), [37] Ni NPs in hydrogel network (25 % activity loss after 5 recycling times) [38], and Ag/CH−FP (10 % activity loss after 4 recycling times) [39], the 40AuNP/Sponge catalyst exhibited significantly better reusability. It was probably because the PU sponge could reduce the chances of leaching and aggregation for AuNPs.

The catalyst exhibited lower and lower efficiency after each recycling time. Therefore, the waste catalyst formed if the catalytic efficiency could not satisfy the requirement. In this work, it was defined as the waste catalyst when the fresh 40AuNP/Sponge catalyst was reused for 8 times, and the regeneration capacity was investigated. For the regeneration of the waste catalyst, 2 mg, 4 mg and 6 mg (5 %, 10 % and 15 % of Au amounts for the fresh catalyst, respectively) $HAuCl_4{\cdot}3H_2O$ were added into 3 mL ultrapure water, respectively. While the waste catalyst was compressed to eliminate air bubbles, an appropriate amount of $NaBH_4$ was added into 5 mL ultrapure water to obtain the solution. Then, the $HAuCl_4$/waste catalyst was added into the $NaBH_4$ solution rapidly and kept vigorous stirring by a vortex mixer for 30 min. At last, the resulted sample was washed and vacuum dried to obtain the regenerated 40AuNP/Sponge catalyst (hereafter denoted as a waste catalyst, 5 % Au regeneration, 10 % Au regeneration and 15 % Au regeneration, respectively).

Figs. 4 and S5 showed the catalytic performance of the waste catalyst and regenerated catalysts for the 2-NA conversion. As shown in Fig. 4, the 2-NA conversion of waste catalysts could reach nearly 100.0 % within 3 min and its apparent rate (k value) was 0.0262 s^{-1}. In contrast, all the regenerated catalysts could finish the reaction within 2 min, and their k value recovered to 0.0362 s^{-1}, 0.0406 s^{-1}, and 0.0444 s^{-1}, respectively. In consideration of economic and catalytic efficiency, 10 % Au regeneration was chosen as the optimal regeneration condition, which was similar to that of the catalyst at the third recycling time. There were two possible reasons for the decrease of the catalytic efficiency after a few recycling times: (1) aggregation of Au nanoparticles; (2) the loss of a small amount of AuNPs from the PU sponge. The waste catalyst could recover higher catalytic efficiency by loading a small quantity of Au, but it was found that the efficiency of the regenerated catalyst could not be as high as that of a fresh one. Furthermore, the catalytic performance of the 40AuNP/Sponge in a flow-through mode was investigated and the result was shown in Fig. S6. It can be seen that the catalytic efficiencies of 2-NA over 40AuNP/Sponge reached about 100 % even if the injection speed was at 0.5 mL·min^{-1}, which was higher than that of AuNPs-anchored paper [40]. In summary, the AuNP/Sponge catalyst exhibited outstanding reusability and regeneration capacity, even though a slight decrease in catalytic efficiency was observed.

3.2. Catalytic reduction for 4-NP

Similarly, we also tested the catalytic performance of the Au/PU sponge on the catalytic reduction of 4-NP. In this experiment, the yellow color of 4-NP/$NaBH_4$ solution faded and bleached ultimately with the addition of the AuNP/Sponge catalyst. The fading time decreased with the increase of the AuNPs amount, and the effect of the AuNPs amount on the catalytic efficiency was then systematically investigated by using UV–vis spectrophotometry (Figs. 5 and S7). The peak intensity at 400 nm decreased and the one at 295 nm increased gradually with the increase of time. Fig. S8 demonstrated the peak position shifted from 315 nm to 400 nm, when the $NaBH_4$ was added into the 4-NP solution. The peak at 400 nm represented 4-NP and the peak at about 295 nm was attributed to 4-AP, as reported from other studies. [41,42] Consequently, the change of peak intensity was triggered by the transformation from 4-NP to 4-AP, when the AuNP/Sponge catalyst was added into 4-NP/$NaBH_4$ solutions.

Fig. 5(b) displayed the 4-NP conversion by AuNP/Sponge with different AuNPs amounts. The conversion rate of 60AuNP/Sponge could reach 79.8 % within 1 min and nearly 100.0 % within 4 min. This conversion rate was satisfactory and higher than that of many studies

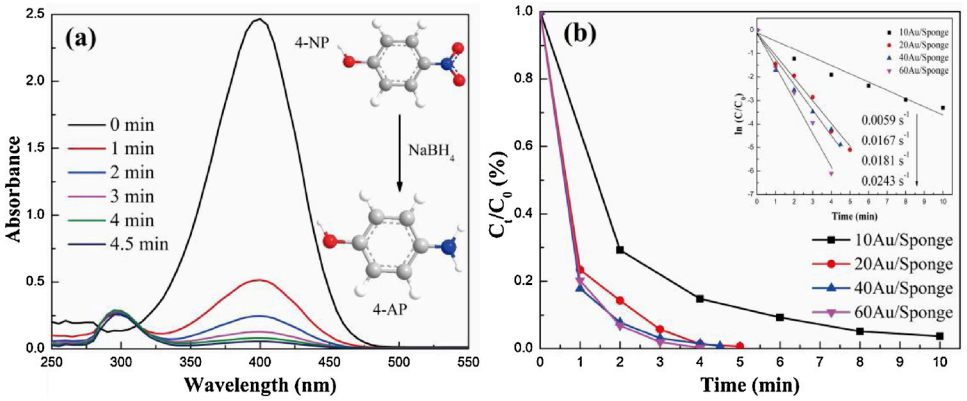

Fig. 5. (a) UV–vis absorption spectra of 4-NP reduction over 40AuNP/Sponge catalyst, and (b) C_t/C_0 vs. time plot.

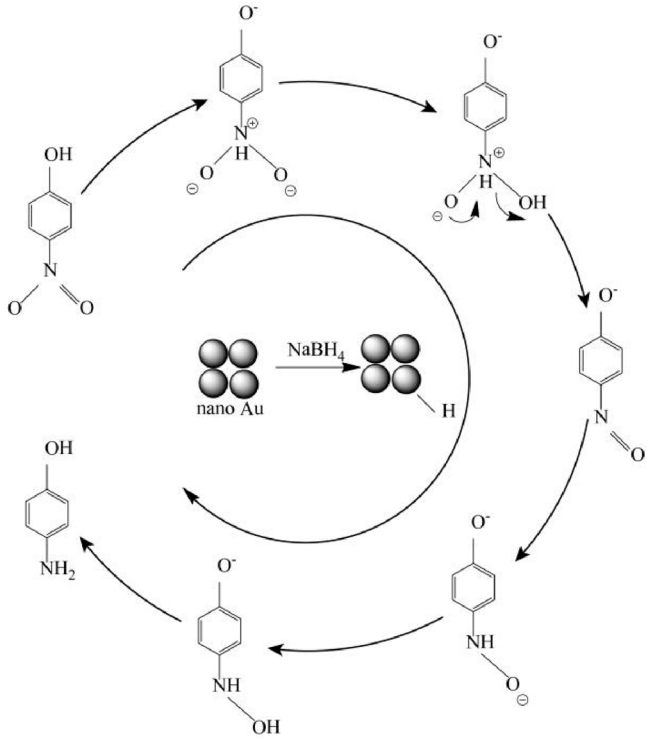

Scheme 2. Proposed reaction mechanism of 4-NP transformation to 4-AP.

[43]. As shown in Scheme 2, the transformation from 4-NP to 4-AP was a six electron process in the presence of $NaBH_4$ [41]. AuNPs on the PU sponge transferred $NaBH_4$ to active hydrogen species adsorbed on the catalyst surface. Afterward, the nitro groups of 4-NP molecules presented in the interfacial region would be transferred to amino groups with the induction of adsorbed hydrogen species [44]. In addition, it was reported that the transformation from 4-NP to 4-AP was thermodynamically favorable but kinetically unfavorable without the catalyst [41]. In other words, AuNPs were the key active component and the AuNPs amount played an important role in the catalytic reduction reaction. As a consequence, the catalytic efficiency decreased gradually when the AuNPs amount reduced on the AuNP/Sponge catalyst. However, the conversion rate of the 40AuNP/Sponge catalyst could also reach 100.0 % within 4.5 min, which was still excellent for catalytic reduction. Fig. 5(b) also displayed the first-order kinetic curves of 4-NP over AuNP/Sponge with different amounts of AuNPs. Similar to the result of 2-NA, it could be seen that the data points followed linearity as well, which was due to the excess $NaBH_4$ in the reaction solution. The values of k were 0.0243, 0.0181, 0.0167, and 0.0059 s^{-1} for the

Table 1
Catalytic efficiency comparison in 4-NP conversion.

Category	Example	k (min^{-1})	Time (min)
platinum-based	FeAgPt alloy [40]	10.06×10^{-2}	25
gold-based	Au/TiO_2 [41]	63.26×10^{-2}	6
silver-based	Ag/Filter paper [34]	23.40×10^{-2}	~12
nickel-based	Ni@PtNi NCs-rGO [42]	27.00×10^{-2}	10
This work	**AuNP/Sponge**	$\mathbf{10.86 \times 10^{-1}}$	**4.5**

60AuNP/Sponge, 40AuNP/Sponge, 20AuNP/Sponge, and 10AuNP/Sponge, respectively. Considering that both the efficiency and economy were significant factors in practical application, the 40AuNP/Sponge was chosen as the optimum catalyst. Furthermore, we calculated the k value and made a comparison with reported values from previous studies (Table 1) [45–47]. The k value of 40AuNP/Sponge was also higher than those of many solid-phase catalysts.

3.3. XRD analysis

XRD patterns of PU sponge and AuNP/Sponge catalyst were analyzed and the results were demonstrated in Figs. 6 and S9. All the reflections of the samples provided the diffraction patterns for the $CaMg(CO_3)_2$ (PDF-ICDD 75–1656) and Au (PDF-ICDD 04-0784). The broad amorphous peak (spanned at 10–30 °) corresponded to the polyurethane in the sponge. As shown in Fig. 6 and Fig. S9, for the PU sponge, the three strong peaks at 2θ = 30.96°, 41.17°, 51.09° were attributed to (104), (11-3) and (11-6) diffractions, respectively. It was suggested that the PU sponge consisted of the amorphous polyurethane

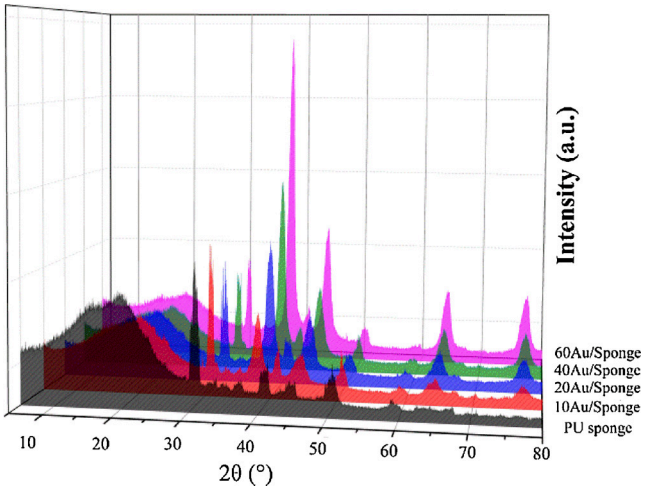

Fig. 6. X-ray diffraction patterns of different catalyst samples.

and crystalline dolomite (the main component was $CaMg(CO_3)_2$). For the AuNP/Sponge catalyst, the obvious Bragg reflections of Au were observed and the three strong peaks at 2θ = 38.25°, 44.46°, 77.72° were attributed to (111), (200) and (311) diffractions, respectively. The strongest peak intensity ratio of Au/$CaMg(CO_3)_2$ increased gradually because the relative amount of $CaMg(CO_3)_2$ decreased with the increase of the AuNPs amount. In addition, the diffraction peaks of $CaMg(CO_3)_2$ shifted to a higher-angle region, while Au peaks shifted to a lower-angle region, implying that the unit cell volume of Au swelled and that of $CaMg(CO_3)_2$ shrank with the increase of AuNPs amount. In other words, there was a strong interaction between AuNPs with $CaMg(CO_3)_2$. Furthermore, the peak intensity and half-peak width of $CaMg(CO_3)_2$ had no noticeable changes, implying that the structure of PU sponge did not change after the AuNPs preparation process, which was significant for the reuse and regeneration of the catalyst.

3.4. FT-IR analysis

It is well accepted that polyurethane was capable of forming several kinds of hydrogen bonds due to the presence of a donor N—H group and a C═O acceptor group in the urethane linkage [48]. These bands have been widely used to characterize the presence of polyurethane. Fig. 7 showed FT-IR spectra of PU sponge and AuNP/Sponge catalyst ($750-4000\ cm^{-1}$), where both spectra were similar to each other and all the peaks were attributed to polyurethane. The band at $3275\ cm^{-1}$ was assigned as -NH stretching in the urethane group and the band spanned at $2700-3000\ cm^{-1}$ was assigned as the —CH stretching [49]. The band at $1716\ cm^{-1}$ and at $1637\ cm^{-1}$ (spanned at $1620-1750\ cm^{-1}$) was assigned as the C═O stretching vibration (amide I). The band at $1532\ cm^{-1}$ (spanned at $1500-1550\ cm^{-1}$) was assigned as the amide II (C—N stretching and N—H bending) [50]. The band at $1221\ cm^{-1}$ (spanned at $1200-1250\ cm^{-1}$) was assigned as the amide III (C—N stretching and N—H bending) and the band at $1080\ cm^{-1}$ (spanned at $1000-1150\ cm^{-1}$) was assigned as C—O—C asymmetric stretching [51]. In addition, all the bands decreased gradually, which was mainly due to the relative amount of polyurethane decreased with the increase of the AuNPs amount. However, there was no peak shift, suggesting that the AuNPs preparation process did not alter the original interactions among PU sponge. In other words, the structure of PU sponge had no change after the AuNPs preparation process, which was beneficial to maintain the catalytic efficiency after 5 recycling times.

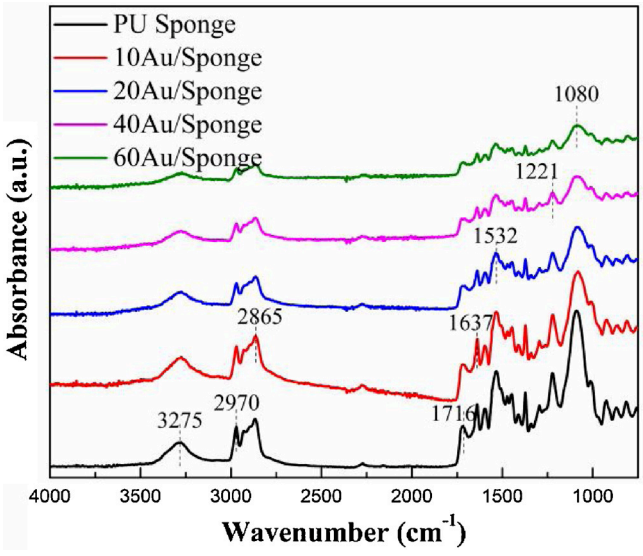

Fig. 7. FT-IR spectra of different catalyst samples.

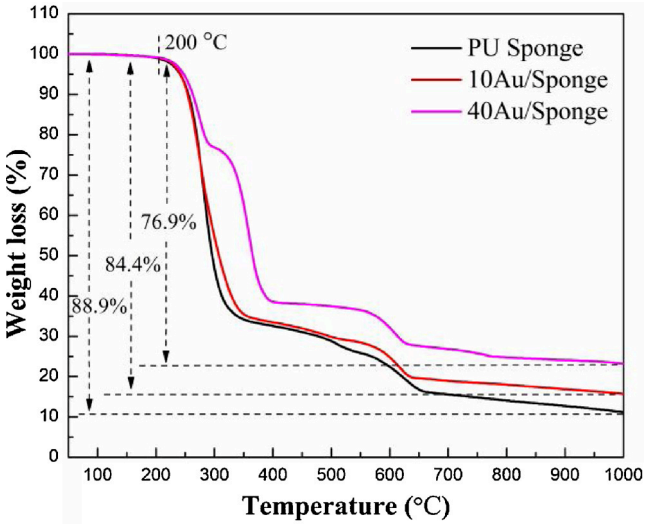

Fig. 8. TGA thermograms of PU sponge and AuNP/Sponge catalysts.

3.5. TGA analysis

Figs. 8 and S10 displayed the TGA and DTG thermograms of PU sponge and Au/Sponge catalyst. From the literature, there were three basic mechanisms for the thermal degradation of the polyurethane: (1) urethane bond dissociation into basic components; (2) breaking of the urethane with the formation of primary amine; (3) splitting the urethane bond into secondary amine and carbon dioxide [52]. There was no weight loss when the temperature increased to 200 °C. It was due to the sample was dried before each test so that moisture was eliminated. All the samples had three stages of degradation: the first stage spanned at 200 – 400 °C; the second stage spanned at 400 – 550 °C and the third stage spanned at 550 – 700 °C. It could be speculated that the first stage degradation was led by the polyurethane phase, the second stage was resulted from a soft segment and the third stage was due to the CaMg $(CO_3)_2$.

The thermal stability could be expressed by the thermal index while the first and second stages of AuNP/Sponge needed a higher temperature for the degradation than that of PU sponge. In consequence, it could be speculated that the AuNP/Sponge catalyst had higher thermal stability than the PU sponge. The improvement in thermal stability can be attributed to the presence of strong interaction between the AuNPs with the PU sponge. The slight shift of the third stage may be resulted from the higher thermal conductivity of AuNPs than that of polyurethane. At last, the weight loss of PU sponge expanded to 88.9 % while that of 10AuNP/Sponge and 40AuNP/Sponge increased to 84.4 % and 76.9 %, respectively. The difference was due to the existence of AuNPs in the PU sponge. Therefore, the amount of AuNPs in the PU sponge could be deduced by the difference of the weight loss and the contents of AuNPs in these three samples were 0 %, 5 %, and 14 %, respectively. This suggested there was a loss of AuNPs during the process.

3.6. XPS analysis

The surface composition and oxidation states of catalysts played an important role in the catalytic reduction reaction, so XPS was tested to investigate the surface properties of the catalysts. XPS analysis also further verified the formation of the AuNP/Sponge catalyst and the efficient removal of oxygenated functional groups of the catalysts. Fig. 9 and Fig. S11 demonstrated the survey, C 1*s*, O 1*s* and Au 4*f* XPS high-resolution spectra of PU sponge and AuNP/Sponge catalysts. From Fig. S11, it could be seen that the PU sponge mainly consisted of C and O elements. On the other hand, for the 10AuNP/Sponge and 40AuNP/

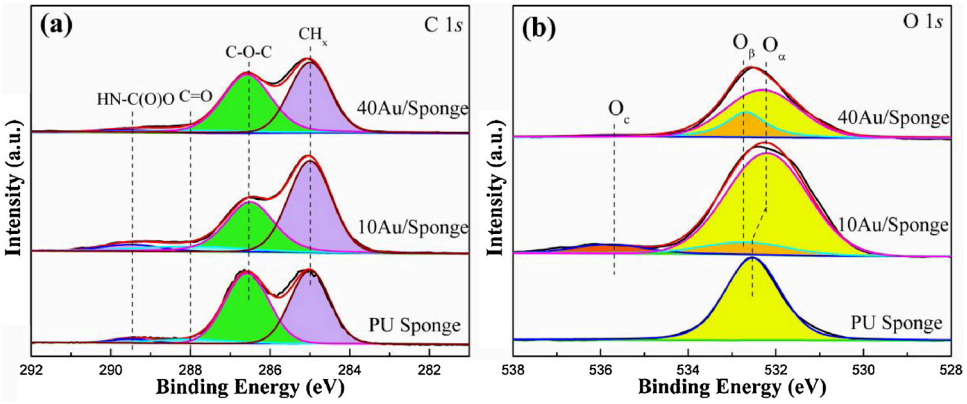

Fig. 9. (a) C 1*s* and (b) O 1*s* XPS high-resolution scan spectra of PU sponge and AuNP/Sponge catalysts.

Sponge catalysts, the strong doublet peaks of Au 4*f* emerging at 87.6 eV and 84.0 eV were attributed to Au° $4f_{5/2}$ and Au° $4f_{7/2}$, respectively. [53] There was also no other peak ascribed to Au^{3+}, illustrating that the reduction of Au^{3+} to Au° was complete during the catalyst preparation. In addition, some peaks attributed to Na element were observed in the AuNP/Sponge catalysts, which was resulted from the $NaBH_4$ during the catalyst preparation. These observations revealed that Au° was the predominant species in AuNP/Sponge catalyst.

Fig. 9(a) showed the representative C 1*s* spectra for the PU sponge and AuNP/Sponge catalysts. All of them exhibited four peaks: (1) the peak located at 285.0 eV was the aliphatic carbon (CH_x); (2) the peak located at 286.5 eV was ether (C—O—C); (3) the peak located at 288.0 eV was carbons bond to a single oxygen (C═O, carbonyl); (4) the peak located at 289.5 eV was carbons bond to two oxygen atoms (O—C = O, carbamide) [54]. The intensity of the C—O—C peak decreased, which was consistent with reduced alcohol (C—OH) surface functionalization. It suggested that the AuNPs consumed the hydroxyl groups of PU sponge and formed strong interaction between AuNPs and the PU sponge. Fig. 9(b) demonstrated the O 1*s* spectra for the PU sponge and AuNP/Sponge catalysts. For the PU sponge, it was composed of a single broad peak centered at 532.5 eV (O_α). When the AuNPs were used to modify the PU sponge surface, a new peak attributed to C—OH surface groups was observed (O_β). This new carbon and oxygen surface environment formed by the strong interaction between AuNPs and C—O—C groups. Moreover, the peak located at 535.8 eV may be attributed to the presence of adsorbed hydroxide (OH^-, O_c) [55,56]. At last, there was a strong interaction between Au and O atoms so that the O 1*s* peaks of AuNP/Sponge showed a shift toward lower binding energy after the catalyst preparation. The strong interaction also guaranteed high reusability of the AuNP/Sponge catalyst.

Table 2 showed the atomic ratios of PU sponge and AuNP/Sponge catalysts. It could be seen that the AuNPs amount of 40AuNP/Sponge was higher than that of 10AuNP/Sponge. This trend was consistent with the TGA results. However, the AuNPs' amount of XPS results was lower than that of TGA results. It suggested that more AuNPs have been generated in the sponge interior.

Table 2
Atomic ratios of PU sponge and AuNP/Sponge surfaces.

Sample	C (At.%)	O (At.%)	Au (At.%)
PU sponge	72.69	27.31	0
10AuNP/Sponge	61.86	35.28	2.86
40AuNP/Sponge	69.48	27.46	3.06

3.7. SEM analysis

Fig. 10 demonstrated SEM micrographs of fresh and used 40AuNP/Sponge (used for 5 times) catalysts. As shown in Figs. 10(a) and S12, the fresh 40AuNP/Sponge consisted of nano polyurethane sponge and the sponge had loose structures. After the measurement, the diameter of the sponge was about 20 − 40 nm. The AuNPs grew along the surface of the polyurethane sponge. The structure of 40AuNP/Sponge became compact gradually and the AuNPs aggregated after 5 times of use. Comparing Fig. S12 with Fig. S13, it could be seen that the used catalyst was brighter than the fresh one, which was due to a small amount of AuNPs separated from the PU sponge during use so that the electrical conductivity of the sample became poorer. The aggregation of AuNPs and the separation of a small amount of AuNPs probably were the main reasons that the catalytic activity decreased gradually after repeated recycling times. Fortunately, the 40AuNP/Sponge still exhibited excellent catalytic performance after many recycling times.

4. Conclusions

In this work, an Au/PU sponge catalyst platform was fabricated via a facile one-step method for efficient catalysis with high reusability. The PU sponge and the AuNP/Sponge catalysts were structurally and morphologically characterized by XRD, TGA, SEM, FT-IR, and XPS, respectively. The AuNPs grew along the surface of polyurethane sponge evenly and the PU sponge consisted of nano polyurethane. The AuNP/Sponge platform exhibited excellent catalytic performance for transforming a nitro group into an amino group. The conversion rate of 2-NA reached nearly 100.0 % within 1.5 min and 4-NP was catalytically reduced completely within 4.5 min by the 40AuNP/Sponge catalyst. Furthermore, the PU sponge could maintain its 3D structure during the AuNPs preparation process, and form a strong interaction with AuNPs, which enabled high reusability of the AuNP/Sponge catalyst. Therefore, this high-efficiency AuNP/Sponge catalyst platform with high reusability can have great potential for various practical environmental and other catalytic applications [57].

Acknowledgments

We would like to acknowledge the financial support from the U.S. NSF-PREM program (DMR 1827745) and Philadelphia Foundation. We are also grateful to the financial support from the National Institute of Allergy and Infectious Disease of the NIH (R21AI107415), Postgraduate Research & Practice Innovation Program of Jiangsu Province (KYCX18_1078), and the Medical Center of the Americas Foundation.

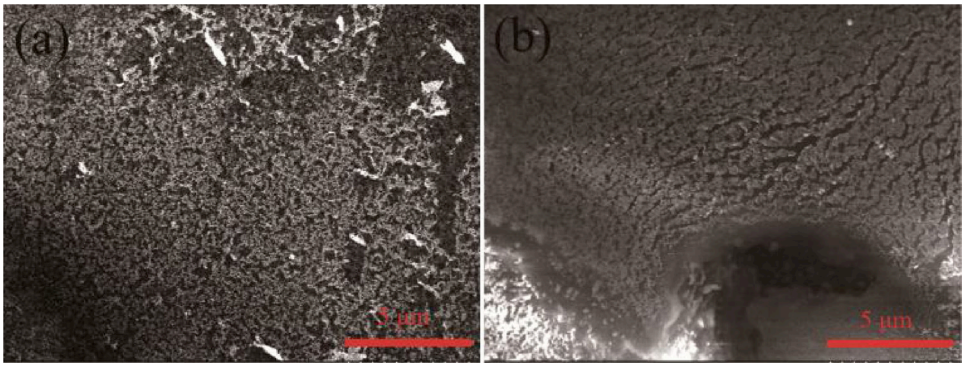

Fig. 10. SEM micrograph of (a) fresh 40AuNP/Sponge and (b) used 40AuNP/Sponge catalysts.

Appendix A. Supplementary data

Supplementary material related to this article can be found, in the online version, at doi:https://doi.org/10.1016/j.cattod.2020.01.023.

References

[1] M. Dou, J.M. Garcia, S. Zhan, X. Li, Chem Comm 52 (2016) 3470–3473.
[2] X. Wei, W. Zhou, S.T. Sanjay, J. Zhang, Q. Jin, F. Xu, D.C. Dominguez, X. Li, Anal. Chem. 90 (2018) 9888–9896.
[3] G. Fu, S.T. Sanjay, W. Zhou, R.A. Brekken, R.A. Kirken, X. Li, Anal. Chem. 90 (2018) 5930–5937.
[4] S. Zhan, H. Zhang, Y. Zhang, Q. Shi, Y. Li, X. Li, Appl. Catal. B 203 (2017) 199–209.
[5] A. Wong, Q. Lin, S. Griffin, A. Nicholls, J.R. Regalbute, Science 358 (2017) 1427–1430.
[6] D. Lopez-Tejedor, R. Benavente, J.M. Palomo, Catal. Sci. Technol. 8 (2018) 1754–1776.
[7] Y. Liu, S.L. Liu, Y. Wang, Q.H. Zhang, L. Gu, S.C. Zhao, D.D. Xu, Y.F. Li, J.C. Bao, Z.H. Dai, J. Am. Chem. Soc. 140 (2018) 2731–2734.
[8] G.X. Zhao, H.M. Liu, J.H. Ye, Nano Today 19 (2018) 108–125.
[9] S.T. Sanjay, W. Zhou, M. Dou, H. Tavakoli, L. Ma, F. Xu, X. Li, Adv. Drug Deliv. Rev. 128 (2018) 3–28 (*Five-Year impact factor 17.23.
[10] M. Thomas, M.U.D. Sheikh, D. Ahirwar, M. Bano, F. Khan, J. Colloid Interf. Sci. 505 (2017) 115–129.
[11] C.M. Cirtiu, A.F. Dunlop-Brière, A. Moores, Green Chem. 13 (2011) 288–291.
[12] S. Rostamnia, E. Doustkhah, Z. Karimi, S. Amini, R. Luque, ChemCatChem 7 (2015) 1678–1683.
[13] P. Garcia, M. Malacria, C. Aubert, V. Gandon, L. Fensterbank, ChemCatChem 2 (2010) 493–497.
[14] S.K. Katla, J. Zhang, E. Castro, R.A. Bernal, X.J. Li, ACS Appl. Mater. Inter. 10 (2018) 75–82.
[15] A.S. Hashmi, G.J. Hutchings, Angew. Chem. Int. Ed. Engl. 45 (2006) 7896–7936.
[16] M.-Q. Yang, X. Pan, N. Zhang, Y.-J. Xu, CrystEngComm 15 (2013) 6819–6828.
[17] Q. An, M. Yu, Y.T. Zhang, W.F. Ma, J. Guo, C.C. Wang, J. Phys. Chem. C 116 (2012) 22432–22440.
[18] Z. Wu, D.E. Jiang, A.K. Mann, D.R. Mullins, Z.A. Qiao, L.F. Allard, C. Zeng, R. Jin, S.H. Overbury, J. Am. Chem. Soc. 136 (2014) 6111–6122.
[19] H.L. Jiang, B. Liu, T. Akita, M. Haruta, H. Sakurai, Q. Xu, J. Am. Chem. Soc. 131 (2009) 11302–11303.
[20] T.J. Corrie, L.T. Ball, C.A. Russell, G.C. Lloyd-Jones, J. Am. Chem. Soc. 139 (2017) 245–254.
[21] D. Han, Z. Bao, H. Xing, Y. Yang, Q. Ren, Z. Zhang, Nanoscale 9 (2017) 6026–6032.
[22] A. Kimura, H. Hayama, J.-y. Hasegawa, H. Nageh, Y. Wang, N. Naga, M. Nishida, T. Nakano, Polym. Chem. 8 (2017) 7406–7415.
[23] N. Wang, X.F. Li, J. Yang, Y.X. Shen, J. Qu, S. Hong, Z.Z. Yu, RSC Adv. 6 (2016) 88897–88903.
[24] X.J. Yang, P.F. Tian, C.X. Zhang, Y.Q. Deng, J. Xu, J.L. Gong, Y.F. Han, Appl. Catal. B 134-135 (2013) 145–152.
[25] X.J. Yang, P.F. Tian, H.L. Wang, J. Xu, Y.F. Han, J. Catal. 336 (2016) 126–132.
[26] Y.F. Han, N. Phonthammachai, K. Ramesh, Z.Y. Zhong, T. White, Environ. Sci. Technol. 42 (2008) 908–912.
[27] T. Zeng, K.L. Ziegelgruber, Y.P. Chin, W.A. Arnold, Environ. Sci. Technol. 45 (2011) 6814–6822.
[28] N. Ullah, M. Imran, K. Liang, C.Z. Yuan, A. Zeb, N. Jiang, U.Y. Qazi, S. Sahar, A.W. Xu, Nanoscale 9 (2017) 13800–13807.
[29] Q.J. Jin, Y.S. Shen, X.J. Li, Y.W. Zeng, Mol. Catal. 480 (2020) 110634.
[30] P. Deka, R.C. Deka, P. Bharali, New J. Chem. 38 (2014) 1789.
[31] V.K. Gupta, M.L. Yola, T. Eren, F. Kartal, M.O. Çağlayan, N. Atar, J. Mol. Liq. 190 (2014) 133–138.
[32] D. Lamey, O. Beswick, F. Cárdenas-Lizana, P.J. Dyson, E. Sulman, L. Kiwi-Minsker, Appl. Catal. A 542 (2017) 182–190.
[33] P.-T. Huong, B.-K. Lee, J. Kim, C.-H. Lee, Mater. Des. 101 (2016) 210–217.
[34] W. Zhang, G. Wang, Z. He, C. Hou, Q. Zhang, H. Wang, Y. Li, Mater. Des. 109 (2016) 492–502.
[35] M.K. Guria, M. Majumdar, M. Bhattacharyya, J. Mol. Liq. 222 (2016) 549–557.
[36] Y.Y. Yue, H.Y. Liu, P. Yuan, C.Z. Yu, X.J. Bao, Sci. Rep. 5 (2015) 10.
[37] C. Huang, W. Ye, Q. Liu, X. Qiu, ACS Appl. Mater. Inter. 6 (2014) 14469–14476.
[38] N. Sahiner, H. Ozay, O. Ozay, N. Aktas, Appl. Catal. A 385 (2010) 201–207.
[39] I. Ahmad, T. Kamal, S.B. Khan, A.M. Asiri, Cellulose 23 (2016) 3577–3588.
[40] H. Koga, N. Namba, T. Takahashi, M. Nogi, Y. Nishina, ChemSusChem 10 (2017) 2560–2565.
[41] T. Kamal, S.B. Khan, A.M. Asiri, Environ. Pollut. 218 (2016) 625–633.
[42] P.H. Zhang, Y.M. Sui, G.J. Xiao, Y.N. Wang, C.Z. Wang, B.B. Liu, G.T. Zou, B. Zou, J. Mater. Chem. A 1 (2013) 1632–1638.
[43] J. Li, C.Y. Liu, Y. Liu, J. Mater. Chem. 22 (2012) 8426.
[44] J.J. Lv, A.J. Wang, X.H. Ma, R.Y. Xiang, J.R. Chen, J.J. Feng, J. Mater. Chem. A 3 (2015) 290–296.
[45] N. Basavegowda, K. Mishra, Y.R. Lee, J. Alloys. Compd. 701 (2017) 456–464.
[46] Z.H. Ren, H.T. Li, Q. Gao, H. Wang, B. Han, K.S. Xia, C.G. Zhou, Mater. Des. 121 (2017) 167–175.
[47] L.P. Mei, R. Wang, P. Song, J.J. Feng, Z.G. Wang, J.R. Chen, A.J. Wang, J. New, Chem. 40 (2016) 2315–2320.
[48] A. Bahadur, M. Shoaib, A. Saeed, S. Iqbal, EPolymers 16 (2016) 463–474.
[49] C.L. Zhang, J.L. Hu, X. Li, Y. Wu, J.P. Han, J. Phys. Chem. A 118 (2014) 12241–12255.
[50] P. Schuchardt, M. Unger, H.W. Siesler, Spectrochim. Acta A. 188 (2018) 478–482.
[51] C.L. Zhang, J.L. Hu, Y. Wu, J. Mol. Struct. 1072 (2014) 13–19.
[52] S. Oprea, V. Oprea, EPolymers 16 (2016) 277–286.
[53] P.M. More, M.K. Dongare, S.B. Umbarkar, P. Granger, C. Dujardin, Catal. Today 306 (2018) 23–31.
[54] L. Watkins, A. Bismarck, A.F. Lee, D. Wilson, K. Wilson, Appl. Surf. Sci. 252 (2006) 8203–8211.
[55] Q.J. Jin, Y.S. Shen, Y. Cai, L. Chu, Y.W. Zeng, J. Hazard. Mater. 381 (2020) 120934.
[56] J.M. Kelly, R.D. Short, M.R. Alexander, Polymer 44 (2003) 3173–3176.
[57] Q. Jin, Y. Shen, L. Ma, Y. Pan, S. Zhu, J. Zhang, W. Zhou, X. Wei, X. Li, Catal. Today 327 (2019) 279–287.